Physicochem. Probl. Miner. Process., 55(4), 2019, 823-839

http://www.journalssystem.com/ppmp

Physicochemical Problems of Mineral Processing

ISSN 1643-1049
© Wroclaw University of Science and Technology

Received September 17, 2018; reviewed; accepted December 12, 2018

Concentration Characteristics of a Complex Antimony Ore

Ergin Gülcan [1], İlkay B. Can [1], N. Metin Can [1], Levent Ş. Ergün [1]

[1] Hacettepe University, Mining Engineering Department, Mineral Processing Division, 06800, Beytepe, Ankara, Turkey

Corresponding author: ergingulcan@hacettepe.edu.tr (Ergin Gülcan)

Abstract: Selection of a proper concentration method for a sustainable production of antimony metal from an ore deposit has its unique challenges and crucial of importance due to the growing use of antimony compounds and increasing strategic importance. Therefore, detailed laboratory scale beneficiation studies of a complex stibnite ore and modeling & simulation studies based on the experimental results were investigated within this study. Quantitative mineralogical characterization, chemical analyses, sieve tests and the heavy liquid tests were performed in the scope of ore characterization. Froth flotation, gravity concentration, electrostatic separation and ore sorting were conducted to introduce the best possible flowsheet for the individual industrial sample. It was concluded that heavy medium separation would be the only method can be used for subjected stibnite ore. Therefore, four conjectural beneficiation scenarios were tested by simulation studies for the cases proposedly allowing to produce concentrates having 10, 12, 14 and 16% Sb content. Within the simulation studies substantiating the real-life processing operation in terms of realistic performance figures, flowsheet design covered the processing of -10+0.5 mm fraction and relatively fine sizes separately via heavy medium cyclone and shaking tables, respectively. Following the itemized mass and water balances, the simulation results showed that when the grade of the concentrates were requested in between 10-16%, the total recovery of the concentrates changed between 46-49% in case of feeding 1.18% Sb with 20 tones per hour feed rate.

Keywords: Stibnite beneficiation, heavy medium separation, shaking table, electrostatic separation, ore sorting, modelling and simulation

1. Introduction

Although antimony (Sb) has the reputation of being naturally complex due to its tendency of abundance with sulfur, oxides, various other metals (pyrite, arsenopyrite, jamesonite, copper, lead and silver, etc.), and mainstream gangue minerals (quartz, chlorite, calcite and plagioclase, etc.), use of antimony compounds in many applications such as lead-acid batteries, flame-retardants, medical chemistry, ceramics and glass, catalysts, jewelry, alloys, pesticides, semiconductors, etc. makes it material of interest in terms of processing and characterization (Minz, et al., 2013; Anderson, 2012; Multani et al., 2016; Lide, 2007; Rawat and Singh, 1976; Henckens et al., 2016; Gad, 2014; Yellishetty et al., 2017).

A sustainable production of antimony within a reasonable scheme and sufficient product quality is increasingly challenging due to the difficulties in beneficiation of this unique ore. Among over 100 antimony minerals discovered up to date, stibnite (Sb2S3) is extensively prevalent which is commonly accompanied with copper, silver, and lead ores (Filella et al., 2002). Additionally, Butterman and Carlin (2004), and Minz, et al. (2013) reported Sb deposits associated with pyrite, arsenopyrite, jamesonite in China, and sulphides of Pb–Ag–Zn–Cu–Sb and quartz rich veins in Idaho, respectively. Although this complex nature of Sb ore mineralogy has its drawbacks while constructing a comprehensive mineral processing flowsheet, there are consensus reached successful methods applied to many antimony reserves such as selective flotation of stibnite, and hand sorting or/and heavy medium separation prior to flotation (Lager and Forssberg, 1989a; Lager and Forssberg, 1989b; Anderson, 2012). Resulting with

DOI: 10.5277/ppmp19003

its toxic and carcinogenic properties, there is also an increasing focus in removal of antimony from aqueous environment recently (i.e. Sb-flotation water wastes) via methods such as electrocoagulation, superconducting high gradient magnetic separation, ferric chloride coagulation, and CF-UF (coagulation–flocculation–ultrafiltration) (Filella et al., 2002; Zhu et al., 2011; Wu et al., 2010; Du et al., 2014; Qi et al., 2018). Analogously, studies concerning antimony-free air and soil are also subject of the many studies powered by the increasing number of related environmental regulations (Multani et al., 2016; USEPA, 1979; Scinicarielloa et al., 2017; Gad, 2014).

Considering the above-mentioned distresses of handling, processing and controlling the antimony, detailed characterization and planning prior to mineral processing operation become the phases of great importance in order to achieve the best possible recovery resulting with lower release of Sb loses to the environment. Consequently, identifying chemical composition and Sb-bearing minerals in the ore, detailed investigation of mineralogical occurrence and liberation state of Sb in mineral matrices, and deciding the separation strategy accordingly are critical steps to follow, since there is a long-known and proven solid link in between mineralogical inferences and mineral processing performance (Minz, et al., 2013; Lotter, 2011; Lotter et al., 2018; Baum, 2014; Lotter et al., 2011). Therefore, beneficiation of a complex antimony ore was investigated using various methods that take the advantage of physical forces, optical behaviors, conductance, and surface properties of antimony. Detailed chemical analyses and modal mineralogical interferences were examined on elemental and mineral basis within involved particle size ranges, respectively. Physical beneficiation methods benefit the operation specific properties such as Sb mineral density, conductivity, and optical reflectivity of electromagnetic radiation being different from host constitutes (Cardarelli, 2008; Anderson, 2012). Fractional density distribution trend was determined via sink-float tests. Following, physical classification and separation equipment alternatives of hydrosizer, jig, shaking table, Falcon concentrator, ore sorter, electrostatic separator, and heavy medium separator were used either in combination with each other or solely depending on the particle size, mineralogical liberation concerns, and operational convenience in order to obtain best possible recovery. Finally, the modelling & simulation studies based on the successful results of conducted test studies were performed within scope of this study in order to reveal the best possible processing scenario for given problematic antimony ore processing.

2. Materials and methods

2.1. Ore characterization

In the experimental work, run of mine samples from Kütahya- Uşak region of Turkey was studied. In order to investigate the best possible processing scenario, detailed characterization studies of the relatively problematic antimony ore were carried out on physical, chemical and mineralogical basis. Therefore, particle size distribution, size-by-size elemental contents, decisive ore mineralogy, and sink-float behavior related to grain sizes were determined.

Initially, a representative batch from the delivered run-of-mine ore was crushed below 10 mm followed by a subsequent screening for fractional chemical analysis. Weight distributions of the size fractions of -10 mm feed sample and metal distributions as the function of feed particle size fractions are given in Table 1 and Figure 1-a. Approximately, 50% of the sample was reported as finer than 3 mm. It is important to note that the complete elemental analysis was performed by using an X-ray fluorescence (XRF) spectrometer. In order to obtain more definitive information about target Sb content, fractions were additionally analyzed via a wet technique (ICP). The results showed that there were noteworthy differences between XRF and wet Sb assays (Figi et al., 2010). In the decision-making point, the wet assays were considered reliable regarding % Sb content. The results given in Table 1 also showed that the %Sb content increases to some extent at finest size fraction. It is known that the antimony minerals are softer and more fragile than the silicates (Lager and Forssberg, 1989b). Hence, they tend to accumulate at finer size fractions. However, there was no significant differences in Sb assays among size fractions, except -38 μm of which top size was reduced to 10 mm after sample preparation.

Characterization efforts were next focused on mineralogical analysis which was performed using QemSCAN to characterize the type of the antimony bearing and gangue minerals. Considering the fragile nature and critically low contents of Sb, a representative sample was crushed and ground down to 212 μm and then four fractions of -212+106μm, -106+53μm, -53+38μm, and -38+20μm were prepared

via wet sieve analysis for the detailed mineralogical analysis. Size distribution of the feed sample with a top size of 212 µm showed that 90%, 80%, and 50% of the material was reported below 165 µm, 116 µm, and 40 µm, respectively (**Figure 1-b**). For quantitative analysis a QemSCAN instrument (FEI Quanta 650F) was used with two EDX detectors (Bruker 5030 SSD) collecting the spectrum at a of 25-kv accelerating potential. The bulk modal analysis was measured in line scan mode (BMA) and the search for Sb-bearing minerals was performed using the Specific Mineral Search mode (SMS) employing the back scatter electron level of the minerals of interest. Elemental reconciliation was also performed for Si, Fe and Sb by comparing the results of chemical analyses and those estimated from BMA results done by QemSCAN. Modal mineralogy and stibnite liberation trends of the size fractions is given in Table 2. Based on the results, the major mineral in all four size fractions was found to be quartz (>80% by weight). Dolomite, calcite, barite, mica and Fe-oxides/hydroxides/sulfides were the next dominant phases with abundances less than 5% by weight. Additionally, five Sb-bearing minerals were identified: Sb-bearing hydroxide, Sb-bearing oxide, stibnite, Sb-clay, and Sb-bearing Fe oxide.

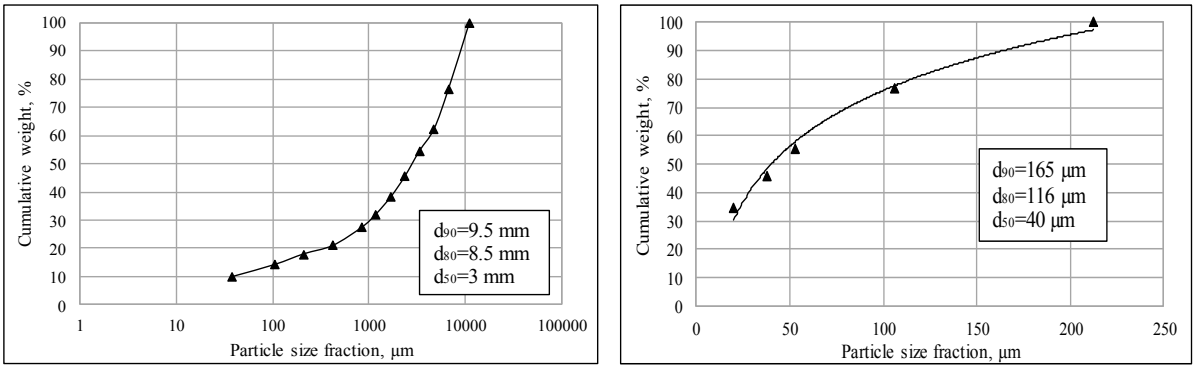

(a) **(b)**

Fig. 1. Feed particle size distributions of the samples below -10 mm (a) and -212 µm (b)

Table 1. Size-by-size chemical analysis of -10 mm run-of-mine ore

		XRF								ICP
Fraction, µm	**Weight%**	**Sb%**	**Si%**	**As%**	**Fe%**	**Cu%**	**Ni%**	**Pb%**	**S%**	**Sb%**
-10000+6700	100.00	0.425	37.25	0.071	0.967	0.011	0.023	0.0001	0.215	0.65
-6700+4750	76.57	1.289	34.74	0.075	1.071	0.012	0.019	0.0001	0.283	1.51
-4750+3350	62.38	1.35	34.55	0.086	1.139	0.011	0.017	0.0001	0.223	1.72
-3350+2360	54.55	1.121	35.5	0.093	1.238	0.013	0.021	0.0001	0.28	1.64
-2360+1700	45.48	1.117	34.05	0.083	1.258	0.012	0.016	0.0001	0.359	1.45
-1700+1180	38.35	1.114	34.06	0.09	1.294	0.011	0.019	0.0001	0.336	1.42
-1180+850	32.02	1.272	34.27	0.085	1.281	0.01	0.024	0.0001	0.374	1.68
-850+425	27.50	1.371	33.27	0.092	1.374	0.012	0.024	0.0001	0.423	1.19
-425+212	21.00	1.409	30.45	0.084	1.371	0.013	0.02	0.0001	0.666	1.65
-212+106	18.00	1.426	32.03	0.059	1.07	0.015	0.019	0.0001	0.894	2.19
-106+38	14.22	1.321	32.02	0.058	1.08	0.058	0.015	0.0001	0.862	1.72
-38	9.88	1.635	27.32	0.151	2.73	0.023	0.009	0.0001	0.485	3.02

In Table 2, it is evident that stibnite presence in liberated form is dispersed to all size fractions tested. On the other hand, the other Sb minerals (Sb-oxide, Sb-hydroxide, etc.) were generally found to be in binary form. Most of binary particles were in the form of Sb-oxide/Sb-hydroxide, and approximately 20% in the form of Sb-oxide/quartz or Sb-hydroxide/quartz. It was also clearly observed in Table 2 that amount of ternary particles was very low indicating high degree of liberation. The major amount of binary particles was only existed in coarsest size fraction and stibnite was found to be binary locked mainly with Sb-oxides minerals. But in finer sizes, this problem was relatively minimized.

In the case of the Sb-hydroxide, the present phase was dominantly Stibconite ($Sb_3O_6(OH)$), which is a product of alteration of stibnite. Half of Sb-Hdyroxides were in 65-95% liberation class. Liberation of

this mineral could only reach up to ~40% at the finest size fraction. A sample chart of QemSCAN association analysis is presented for Sb-hydroxide is given in Figure 2-a.

Table 2. Modal mineralogy analysis results of the -212 μm run-of-mine sample

Modal Mineralogy				
Mineral, Mass (%)	-212+106μm	-106+53 μm	-53+38 μm	-38+20 μm
Stibnite	0.21	0.30	0.25	0.20
Sb-oxide	0.91	0.85	0.69	0.62
Sb-hydroxide	1.80	1.56	1.34	1.43
Sb-Fe-oxide	0.13	0.19	0.16	0.16
Sb-Clay	0.33	0.27	0.23	0.21
Quartz	80.62	82.00	83.05	83.37
Mica	2.42	2.96	2.56	2.35
Olivine	0.09	0.02	0.01	0.04
Kaolinite	0.10	0.12	0.10	0.13
Calcite	2.71	2.62	2.78	2.81
Dolomite	4.86	4.58	4.33	4.20
Rhodochrosite	0.04	0.00	0.01	0.01
Flourite	0.35	0.25	0.25	0.26
Fe-oxide/Hydroxide	1.12	0.81	0.71	0.90
Ti-oxide	0.03	0.06	0.05	0.07
Fe-sulfide	1.08	0.86	0.85	1.00
Barite	2.92	2.28	2.35	1.94
Apatite	0.08	0.04	0.06	0.05
Others	0.20	0.23	0.21	0.25
Total	**100.00**	**100.00**	**100.00**	**100.00**
Stibnite Liberation				
Liberation (%)	-212+106μm	-106+53 μm	-53+38 μm	-38+20 μm
100 % free	47.84	86.32	94.1	91.57
65-95 % free	48.63	9.98	4.44	4.05
35-65 % free	0	3.28	0	3.06
5-35 % free	1.45	0.36	1.13	1.2
0-5 % free	2.09	0.06	0.33	0.12
Total	100	100	100	100

Sb-Oxides and Sb-Hydroxides showed generally binary type of locking rather than ternary form. As the amount of quartz was over 80% in all size fractions, its liberation supposedly played an important role during the planning stage of concentration method. Quartz in the subjected antimony ore was mostly in free form within a liberation class in between 65-95%. While its being underlined that quartz mineral was mostly free, the remaining was in the form of ternary type of locking. Approx. 20-30% of quartz was dispersed in different minerals. Calcite, and Sb-Oxi/Hydro minerals were observed to be the binary associates of quartz. Quartz was mostly associated with calcite and Sb-Ox/Hydro minerals in the binary particles as given in Figure 2-b.

Following the mineralogical analyzes, heavy liquid tests were conducted as part of the characterization studies on the size fractions of -10+3.35 mm, -3.35+1 mm, -1+0.425 mm and -0.425+0.106 mm to ensure the feasibility of gravity concentration. Separation of particles from each other via individual density differences (and thus specific gravity and buoyancy) require controlled particle size fractions in order to minimize the effect of the size on settling. Effect of viscosity on settling behavior increases with decreasing particle size. Therefore, narrow size fractions, considering the amount of material, were prepared and subjected to heavy liquid tests separately in an isolated heavy medium. Additionally, increasing liberation through finer sizes introduces more liberated particles to the system, which allows to maintain a clearer perspective on the ideal gravity separation performance for given

particle size range along with mineralogical liberation analysis. Heavy liquid tests of fine size fractions are usually problematic and inconclusive due to viscosity and possible chemical interactions with the liquid. Hence, -0.106 mm fraction was excluded from the test program. The heavy liquids were prepared at densities of 2.65 g/cm^3, 2.75 g/cm^3 and 2.96 g/cm^3 using mixture of tetrabromoethane and carbon tetra chloride. The procedure of the test sequence is given in Figure 3. The heavy liquid test products and feed were then subjected to drying, weighing, and analyzing for Sb content via wet technique. It was clear that even with -10+3.35 mm size fraction, a concentrate containing 18.1% Sb could be produced at 2.96 specific gravity (Figure 4-a). The recovery in the same size fraction was 42.3% which was corresponding only 9.71% weight of the total sample (Figure 4-b). Similar trend was also observed with the following size fractions. The Sb grade of the sink fractions was similar but the recovery increased proportionally through finer size fractions due to the increasing liberation. The highest recovery value of 82.8% was obtained with the finest size fraction, -0.425+0.106 mm. Based on the results it was concluded that, approximately 46% of Sb can be recovered ideally by gravity concentration from a feed having -10 mm particle size fineness. The Sb grade of the concentrate would be about 18-19%. Moreover, higher recoveries can be obtained at finer particle sizes. In that case, the amount of fine particles (-0.106 mm, 13.86% by weight, 1.55% Sb, 17.82% of overall Sb distribution) is critical considering that the treatment of fine particles with gravity concentration equipment is always considered problematic.

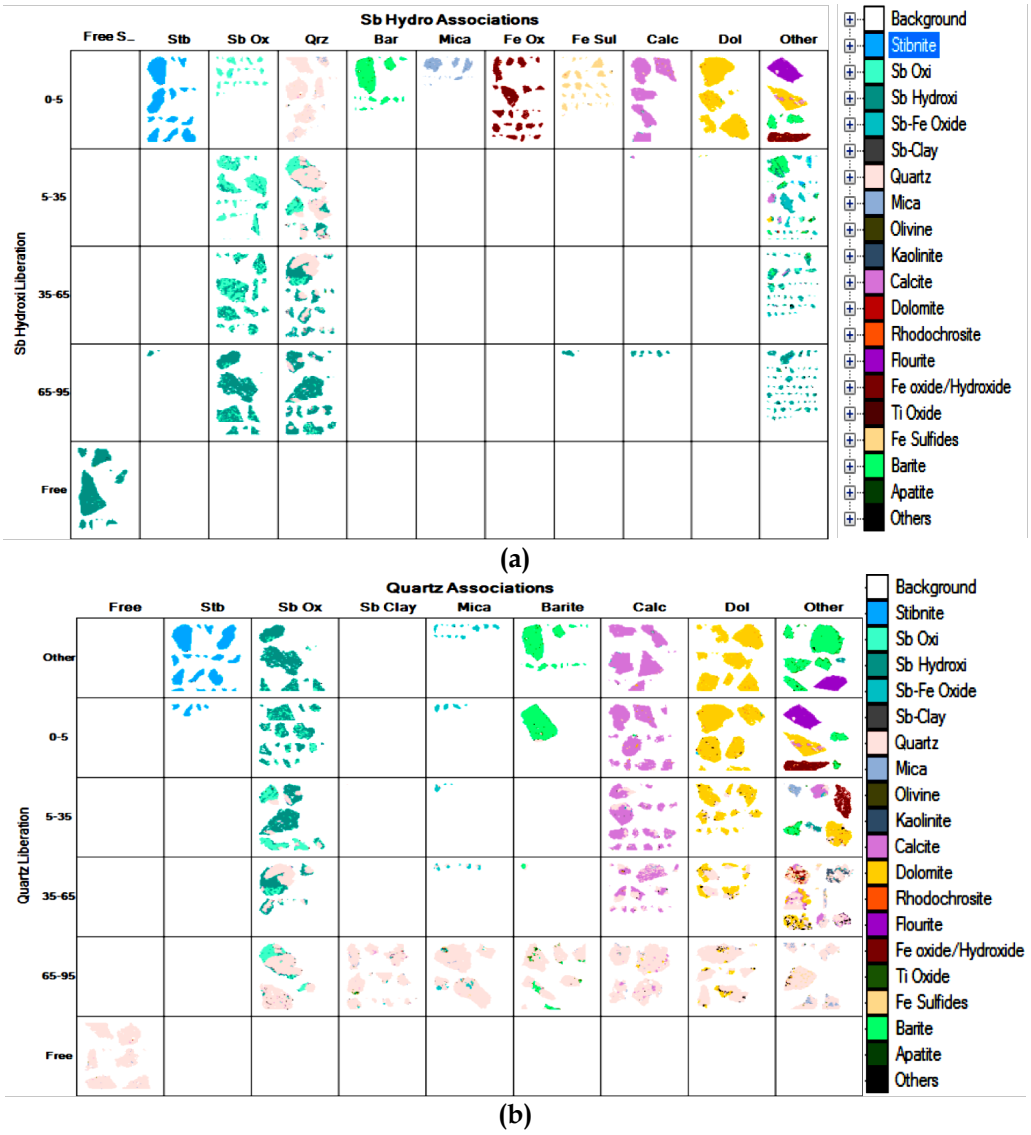

Fig. 2. Sb-Hydroxide (a) and Quartz (b) associations and locking types of the subjected antimony ore (Sb Oxi: Sb-oxide, Sb Hyd: Sb-hydroxide, Qtz: Quartz and/or Si hydroxide, Bar: barite, Cal: calcite, Dol: dolomite)

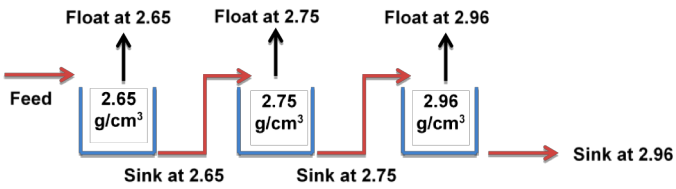

Fig. 3. Schematical procedure of heavy liquid tests

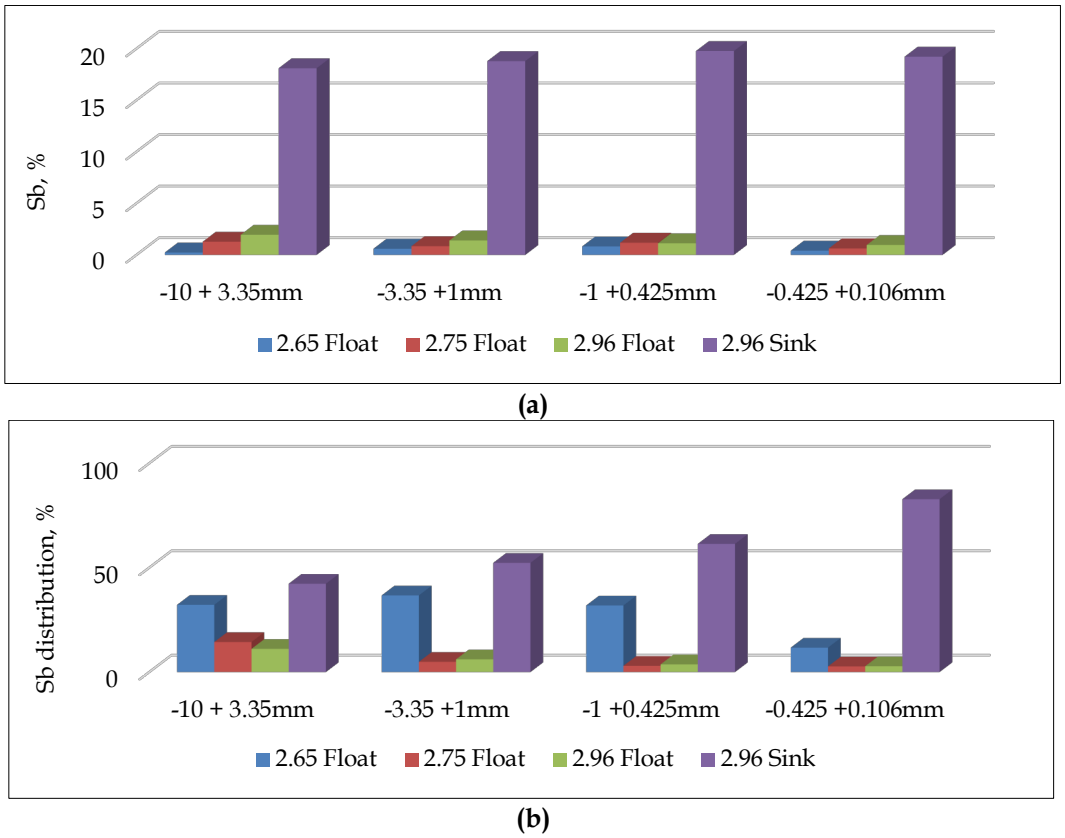

Fig. 4. Size-by-size heavy liquid test results due to % Sb grade (a) and distribution (b)

2.2. Experimental overview

Following the characterization studies, gravity concentration (jig, shaking table, Falcon, and heavy medium), flotation, electrostatic separation and optical sorting tests were designed within specific size fractions, considering the complex mineralogy, clayey content, and liberation status of Sb ore. Experimental designs were determined to obtain a coarse pre-concentrate first, prior to processing relatively fine sizes, in order to minimize the common struggle caused by slimes and clayey contents. Additionally, a sufficient increase in the head grade of feed was aimed before subsequent enrichment methods, as suggested by mineralogical footprints. Considering the upper and lower particle size limitations of gravity powered methods, while relatively coarse sizes were selected in heavy medium and jig aiming to obtain a Sb pre-concentrate with reasonable recovery, finer sizes were selected when processing with Falcon and shaking table aiming to obtain either a Sb pre-concentrate or a final high-grade concentrate with reasonable recovery and without any significant loses to the slimes (Anderson, 2012). Since the slimes in an industrial heavy medium separation is usually lost, a narrow and relatively coarse size fraction was chosen to reach a sufficient pre-concentration performance in accordance with the heavy liquid test results (Bosman, 1998). Mineral jig used in the experimental studies was a classical Harz type laboratory scale setup of which operating range was in between 10 mm and 0.5 mm, since the industrial equipment is eligible to process mineral batches having various particle size ranges from 38.1 mm to 6.35 mm (Gupta and Yan, 2006). Shaking tables are also capable of processing particle size

ranges from 15 millimeters down to 10-15 microns within capacity restrictions and size classification requirements of the given process (Manser et al., 1991). Within the subjected Sb ore, shaking tables were proposedly considered as the final stage of the gravity concentration powered process scheme, and particle size ranges were determined accordingly. On the other hand, Falcon concentrator is more efficient in recovering fine and liberated slime scale particles with the incorporation of high centrifugal forces (Gupta and Yan, 2006). Considering the buildup of an industrial scale process scheme with high capacity, Falcon itself was preferably used to recover Sb from the slimes lost during size classification operations. Similarly, optical sorting tests were considered as a dry pre-concentration alternative to decrease the mass load prior to size reduction of flotation operation. Hence, optical sorting tests were performed with a coarse sample batch representing a primary crusher discharge. While the sorting method could theoretically be performed with a material down to 0.5 mm, then the capacity would decrease to a non-feasible couple of hundred kilograms per hour (Wotruba, 2006; Gordon and Heuer, 2000; von Ketelhodt, 2009). Finally, electrostatic separation was considered as a dry alternative, although the real-life operational predicaments such as dry grinding requirement, low capacity, and operational difficulties were on the table. Therefore, the coarsest top size limit was chosen to the utmost at which liberation emerges slightly in order to obtain a Sb-free tailing.

As one might expect, heavy liquid test results are solid indicators for the feasibility of gravity concentration. Therefore, gravity concentration scenarios were applied considering the use of various gravity based equipment having different performance figures (Wills and Finch, 2015). Also, size classification is essential prior to the gravity concentration due to the increase the effect of density on separation performance. Therefore, a representative portion run-of-mine ore was crushed and ground down to two representative sample batches of -1 mm and -300 µm. A hydrolic classifier (hydrosizer) with four compartments was used to classify the material and remove the slimes from -1 mm and -300 µm sample batches, separately. Although hydrosizer is principally a classifier, relatively higher water rate at first compartment ensure a slightly higher-grade product and coarser particles to accumulate within. With both sample batches, the material in the first two compartments was combined as coarse fraction and the material from 3rd and 4th compartments as fine fraction. The overflow was separated as slime material. Combined hydrosizer compartments of -1 mm and -300 µm feed samples were fed to the shaking tables separately. Schematic view of shaking table tests in combination with hydrosizer is given in Figure 5.

Considering the particle size limitations and to prevent losses to slime product, hydrosizer overflow slime fraction of -1 mm feed was fed to Falcon concentrator. Three stages of subsequent cleaning were performed to obtain a clean product in terms of Sb content. Slime fraction of -300 µm feed was removed without any treatment due to the extreme fineness, low Sb loss, and clayey content which was inadaptable for physical separation via Falcon. As for the jigging tests, representatively sampled -10 mm run-of-mine sample was used without any classification prior to operation due to the particle size limitation of the jigging operation.

Finally, based on the heavy liquid test results, direct heavy medium separation tests were performed using -10+3 mm size fraction at two different medium densities of 2.6 and 2.7 g/cm^3. Heavy media was prepared by mixing high grade magnetite powder (d_{90}=-45 µm) with enough water to reach the desired density. A 30 liters of effective volume, laboratory scale, and vertically positioned heavy medium vessel was operated continuously within the experimental studies. Schematic representation of heavy medium separation tests is given in Figure 6.

Flotation tests were performed using two distinct feed samples. Detailed chemical regime of each flotation practice is given in Table 3. In 1st and 2nd flotation tests, hydrosizer overflow of -1mm feed was processed, while 3rd-8th tests were performed with crushed -2 mm run-of-mine ore after sufficient grinding was applied. Crushing stage was conducted subsequently with Jaw and Roll Crushers, obtaining a sample batch having -2 mm in size (d_{80}= 1.25 mm). Following, crushed -2 mm material was sampled into equal 2 kg sample bathes and ground for 20 minutes with 40% solid by weight, obtaining a final product having d_{80}=75 µm which collaborates the required fineness suggested via liberation analyses results. Hydrosizer overflow stream of -1 mm feed was used in 1st and 2nd flotation tests in order to prevent the overall material loses, and to use the flotation for recovering the Sb loses via slimes complementing the final gravity concentration scheme. The hydrosizer overflow of -1mm feed also

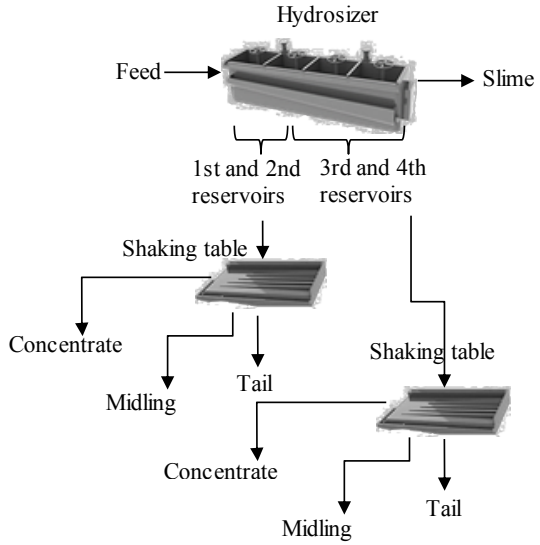

Fig. 5. Schematic representation of shaking table tests

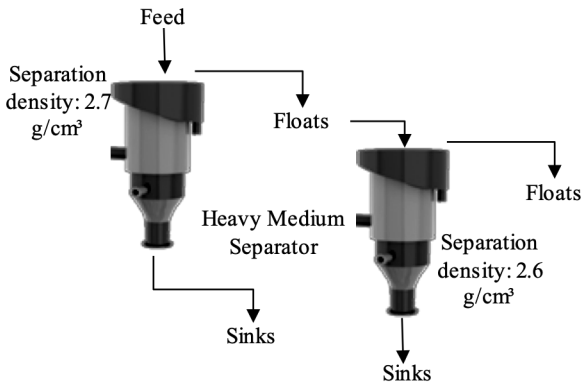

Fig. 6. Schematic representation of heavy medium separation tests

contains high amount of clay which can cause viscosity and slime coating problem in flotation. Therefore, Na-silicate was used for dispersion and depression. Consequently, two tests were performed using the slime material; 1st test to float stibnite, 2nd test to float both stibnite and Sb-oxides by using hydroxamate type collector (industrial $Aero_{6493}$). 3rd-8th flotation tests were conducted with different chemical regimes to increase final product qualities. 3rd test was the base line test, aiming to float stibnite by lead activation. In 4th test, effect of hydroxamate type collector on flotation of Sb-oxides minerals was tested. In 5th test effect of sulphidisation, in 6th test effect of activation by $CuSO_4$, in 7th test effects of Na-oleate:hyroxamate mixture, and in 8th test the use of amin:oleate collector mixtures in the presence of high dosage of NaHS were tested, respectively. In all flotation tests, a standard 2.5-liter flotation cell at approx. 1400 rpm impeller speed was used.

Table 3. Chemical regimes used in flotation tests

	Na silicate	$PbNO_3$	PAX	D_{250}	F_{507}	$Aero_{6493}$	NaHS	$MnCl_2$	$CuSO_4$	Na-Oleat	Amin
						grams/tone					
1st test	1000	1000	100	15	10						
2nd test	1000	500	100	15	10	100					
3rd test	1000	1000	100	15	10						
4th test	1000	1000	100	100	15	10					
5th test	1000	1000	100	15	10		500				
6th test	1000		50	15	10	50		500	500		
7th test	1000	500	50	15	50	50				50	
8th test	1000		100				2000			25	25

It is known that antimony minerals have poor conductivity and they are generally regarded as semi-conductors (Cardarelli, 2008). In order to benefit this property, an electrostatic separation test was conducted on the concentrate product of shaking table which was obtained from first two compartments of hydrosizer when -300µm test sample was processed **(Figure 7)**.

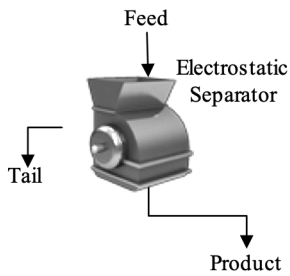

Fig. 7. Schematic view of the tests applied with conventional electrostatic separator

For the optical sorting practices, sample batches having large lump of particles with a narrow particle size range of -35+10 mm were fed to both visible light (VIS) and Near-infrared light (NIR) responsive sensor mounted optical sorters, respectively (Gülcan and Gülsoy, 2018). Schematic views of the optical sorting tests were illustrated in Figure 8a-b. While a single stage sorting was performed with NIR sorting, rejected fraction of first stage VIS sorting was additionally subjected to a second stage cleaning. Additionally, the low infrared radiation absorbing particles were rejected within former, and darker particles were rejected within the latter tests.

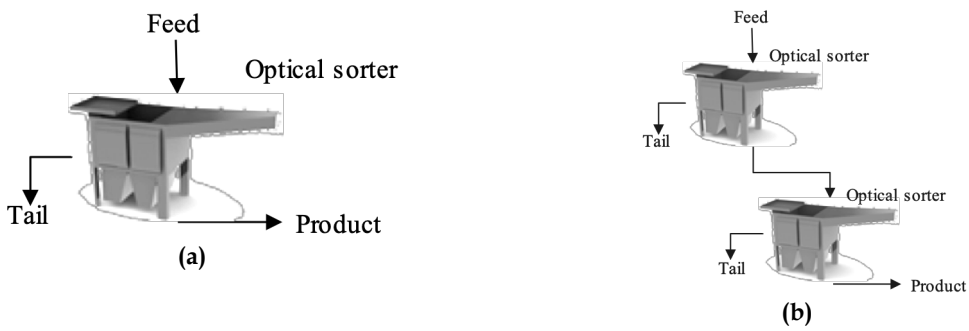

Fig. 8. Schematic view of optical sorting tests applied with Near-infrared (a) and VIS (b) sensors

3. Results and discussion

3.1. Froth flotation tests

Two sets of flotation tests were performed using the hydrosizer overflow material (slime material) and the run-of-mine ore as feed, respectively. The effects of the parameters such as hydroxamate type of collectors for Sb-oxides, sulphidisation, collector mixtures, lead and $CuSO_4$ activation were investigated. The overall results in terms of final products' %Sb content and recovery were given in Table 4. Although various flotation conditions were applied for the flotation of Sb-oxide minerals, results were not successful presumably due to the slime coating. While liberated stibnite particles in the test sample could be floated easily, the low initial amount of stibnite in the ore in combination with the presence of ultra-fine clayey content resulted in with an exhausted system prohibiting selective flotation of the Sb-oxide minerals. Consequently, in the tests performed with hydrosizer overflow, a concentrate having approx. 2.5% Sb grade could be obtained with very low recovery (approx. 8%). Moreover, addition of hydroxamate type collector did not significantly improve the flotation of Sb-oxide minerals.

Similarly, flotation tests performed with run-of-mine sample were also failed despite the application of the offbeat conditions in 8th test which is successfully applied for flotation of Zn-oxide minerals in the industry. The results given in Table 4 showed that the maximum Sb recovery was about 17%.

Consequently, Sb recovery values were failed for this specific antimony ore in terms of considering an enrichment strategy based on froth flotation under given circumstances.

Table 4. Results of the flotation tests applied on the hydrosizer overflow sample

Flotation test notation	Weight (%)	Sb (%)	Sb Recovery (%)	Cumulative Sb (%)	Cumulative Sb Recovery (%)
1st test	4.60	2.40	4.32	2.69	6.27
2nd test	6.29	2.28	5.72	2.39	7.58
3rd test	3.23	6.11	7.52	9.06	16.24
4th test	5.36	4.64	7.75	6.79	15.99
5th test	3.43	6.00	7.78	8.66	15.83
6th test	2.84	10.20	12.35		
7th test	13.05	1.64	7.34	2.09	10.69
8th test	4.60	2.40	4.32	2.69	6.27

3.2. Gravity concentration tests

Various gravity concentration methods covering heavy medium separation, jigging, high centrifugal gravity separation with Falcon concentrator and shaking tables were investigated either in combination with size classification or solely.

-10 mm original sample and – 1 mm combined hydrosizer 3rd and 4th compartments were fed to the jig and Falcon concentrators, respectively. Resulting product for the former was having 1.51% Sb with an insufficient 29.13% Sb recovery, while the latter could hardly achieve 3.15% Sb after three stages of cleaning with an overall Sb recovery of 2.07%. Unfortunately, no appreciable concentration could be able to achieved by jigging and Falcon tests.

Shaking table tests were performed with four individually classified samples of -1mm and -300µm batches. Results of the hydrosizer classification tests applied to -1mm and 300µm run-of-mine sample batches were presented in Table 5. The amount of coarse fraction of -1 mm feed was 41.5% with 1.47% of Sb content. Nearly half of the material was reported to slime fraction with 1.72% Sb content. On the other hand, 60% of the -300 µm feed material was reported in the first two compartments of hydrosizer, while only 9% of it was collected from the combination of 3rd and 4th compartments. The weight of slime fraction for -300 µm feed material was recorded as 31% (Table 5). Products in the 1st and 2nd compartments of the hydrosizer obtained from -1 mm and -300µm feed materials were combined and fed to the shaking table as coarse fraction, separately. Similarly, 3rd and 4th compartments were combined and fed to the shaking tables as fine fractions. Results of the shaking table tests applied to coarse and fine fractions of the hydrosizer operation performed with -1 mm and -300µm feed materials were given in Table 6. Only ~27% of -1 mm feed material was recovered as concentrate with a Sb grade of 2.52%. The best result of the shaking table tests was no more than ~50% recovery with a concentrate of 3.15% Sb content which was given in Table 6. The majority of the materials was obtained as middling and tail. The fine fraction obtained from the combined 3rd and 4th compartments of the hydrosizer offered better results rather than the coarse fraction of -1mm feed material. The grade and the recovery of the concentrate were increased slightly due to decreasing particle size and probably liberation, but it was obvious that the results need to be improved. As for the -300µm feed material, the recovery of the concentrate was recorded as 43.5% with 3.12% Sb grade. Although the mass pull of the middling was also higher in comparison with -1mm feed material, it was hard to consider combining it with the concentrate since its grade was also rather low. Additionally, an unacceptable portion of the material was lost with the tailings when the combined of 3rd and 4th hydrosizer compartments of -300 µm feed material was fed to the shaking table.

Final gravity-based concentration effort was conducted with a heavy medium vessel. Heavy medium separation test was performed with a sized -10+3mm feed material at two different medium densities of 2.6 and 2.7 g/cm^3 prepared with -38 µm powder grade magnetite to reach the desired pulp densities. According to the results given in Table 7, the amount of fraction heavier than 2.7 g/cm^3 density was only about 0.5% weight with a Sb grade and recovery of 21.86% and 9.82%, respectively.

Hence, highest grade value could be achieved with heavy medium separation of which results were also corroborated the sink-float test results.

Table 5. Results of the hydrosizer tests applied to -1mm and -300µm run-of-mine test samples

	-1 mm feed sample			-300 µm feed sample		
	Weight (%)	Sb (%)	Recovery (%)	Weight (%)	Sb (%)	Recovery (%)
1st and 2nd Comp.	41.50	1.47	39.71	59.63	1.08	52.86
3rd and 4th Comp.	10.46	0.93	6.33	9.17	0.94	7.03
Hydrosizer Slime	48.05	1.72	53.96	31.20	1.57	40.11
Hydrosizer Feed	100.00	1.53	100.00	100.00	1.22	100.00

Table 6. Results of the shaking table test applied on coarse fraction of -300 µm and -1 mm fraction test sample

	1st and 2nd Comp.			3rd and 4th Comp.		
	Weight (%)	Sb (%)	Recovery (%)	Weight (%)	Sb (%)	Recovery (%)
	-1 mm feed sample					
Concentrate	6.52	2.52	26.99	1.54	3.15	49.95
Middlings	22.47	1.52	56.14	4.31	0.57	25.31
Tailings	12.51	0.82	16.87	4.61	0.52	24.74
Feed	41.50	1.47	100.00	10.46	1.04	100.00
	-300 µm feed sample					
Concentrate	9.00	3.12	43.51	0.51	1.95	11.59
Middlings	45.78	0.70	49.35	0.63	1.35	9.91
Tailings	4.85	0.95	7.14	8.03	0.84	78.50
Feed	59.63	1.08	100.00	9.17	0.94	100.00

Table 7. Results of the heavy medium separation test applied on -10 + 3mm size fraction test sample (-3mm fraction has 1.62%Sb content)

	Weight (%)	Sb (%)	Recovery (%)	Cumulative Sb (%)	Cumulative Recovery (%)
2.7 Sinks	0.5	21.86	9.82	21.86	9.82
2.7 Floats	3.86	1.74	6.09	4.03	15.91
2.6 Floats	95.64	0.97	84.09	1.1	100
Feed	100	1.1	100		

3.3. Electrostatic separation tests

In order to benefit the semi-conductivity of the antimony, an electrostatic separation test was conducted with the concentrate product of shaking table which was obtained from first two compartments of hydrosizer when -300µm test sample was processed. But again, no significant concentration could be

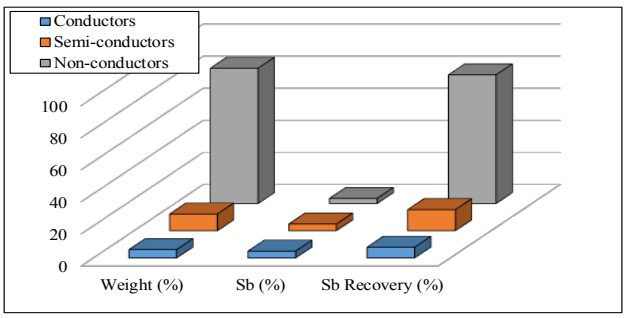

Fig. 9. Results of the electrostatic separation test applied to the concentrate of the shaking table test with coarse fraction of -300µm test sample

able to achieved (Figure 9). The maximum recovery obtained with electrostatic separation of semi-conductor fraction was approx. 13% with a 4.18% Sb grade.

3.4. Optical sorting tests

NIR and VIS sorting practices were applied for pre-concentration purposes. The maximum grade and recovery of the concentrate were obtained with VIS sorting as 3.86% and 28%, respectively, which was not sufficient for conducting a process flowsheet incorporating the ore sorting method. Results of the optical sorting tests were given in Figure 10, along with the product images in Figure 11.

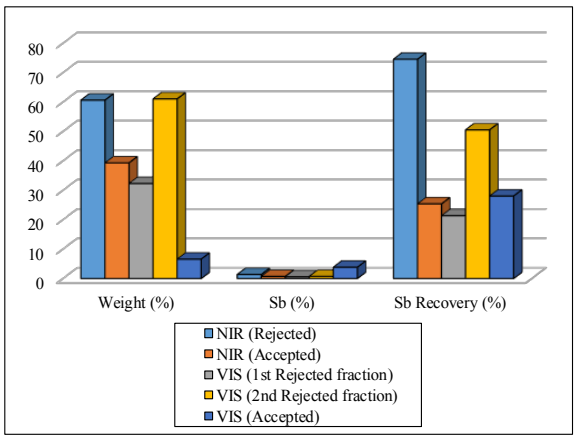

Fig. 10. Results of the optical sorting tests

Fig. 11. Products after separation a) NIR sorting b) Color sorting

3.5. Modelling and simulation studies

Considering the results of the experimental studies, it was decided that heavy medium separation would be more feasible for this specific antimony ore. Therefore, simulation studies were performed to estimate possible operating scenarios. It is important to note that the heavy medium separation equipment, which was proposedly chosen to be used in simulation studies, should be defined by a definite mathematical model.

The density separating performance of a gravity concentration or DMS (dense medium separating) process can be completely described by the partition curve. Partition curves can be evaluated mathematically by Whiten's Efficiency Curve Model (Whiten, 1966; Whiten, 1972a; Whiten, 1972b):

$$\frac{100\,(\exp(\frac{\alpha\rho}{\rho_{50}})-1)}{\exp(\frac{\alpha\rho}{\rho_{50}})+\exp(\alpha)-2} \quad \text{and} \quad \frac{1.099 * \rho_{50}}{E_p}$$

where, P is partition number, expressed as a percentage, A is slope or efficiency parameter, ρ is particle density, ρ_{50} is separation density and E_p is Ecart Probable.

Hence, when Ep and ρ_{50} are known, partition curve can be created and products can be predicted by the model. All gravity separators have their own typical Ep and ρ_{50} values. Exceptionally, ρ_{50} is mainly related to medium density in dense medium applications. For HMS, Ep range is in between 0.02 – 0.06, and for shaking table applications Ep range is in between 0.3 – 0.5 (Mular et al., 2002).
In modelling study, the Ep values for HMS and shaking table are calculated as 0.03 and 0.35 respectively, at a separation density of 2.7 g/cm^3. The separation performances of these equipment used in the simulation studies were determined due to the Ep values given in Figure 12. It was obvious that the performance of HMS indicates a more ideal separation than shaking tables.

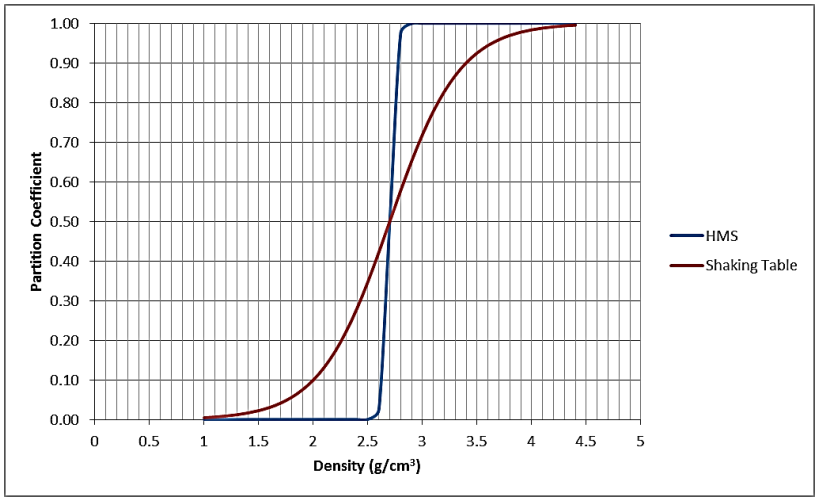

Fig. 12. Comparison of separation performance of HMS and Shaking Table on the same cut density, 2.7 g/cm^3 (Ep_{HMS}: 0.03, Ep_{Table}:0.35)

For simulation studies, the software namely LAVE® was used. In simulations studies, -10 mm feed material was fed to a screen which had an aperture of 0.5 mm. While -10+5 mm material was concentrated via a Heavy Medium Cyclone, -0.5mm fraction was subjected to two stages of shaking table operation. Consequently, conjectural four different scenarios targeted to produce concentrates having 10, 12, 14 and 16% of Sb contents were carried out. The feed rate was taken into account as 20 tons per hour having 1.18% Sb head grade in all simulations. The flowsheet design was kept same, but the flowrates and the grades of the streams were alternated by the model due to the change in concentrate grade. The coarse concentrate was produced from the concentration of -10+5mm fraction with Heavy Medium Cyclone while the fine concentrate was the product of two stages of shaking table operations. It should be noted that no significant changes were occurred in the grades of the slime and tail fractions. When the grades of the concentrates were changed between 10-16%, then the total recoveries of the concentrates were changed between 46-49%. Summary of these simulation scenarios are tabulated in Table 8.

3.6. Effect of ore mineralogy on flowsheet selection based on experimental results

The schematic representation of the mineralogy of the antimony ore which was supported by QEM Scan images is exhibited in Figure 13 in more detail. Since there were fine inclusions of the Sb minerals in the quartz matrix other than the liberated ones, it was not possible to get the required liberation of this inclusions even with the fine grinding. The crack planes indicated on Figure 13 would potentially provoke particles having many different compositions except a liberated one. On the other hand, these

findings were also corroborated the experimental results due to the fact that particles having higher Sb content would have had a higher density than the others. At this point, the success of the gravity concentration application is highly dependent on the extend of the differences in the density of initial particles. Within the case of the beneficiation of the antimony ore discussed through this study, this difference was delicate enough to be considered in some extend when only heavy medium separation was applied. Such liberation profile will not be sufficient for any other beneficiation method. Therefore, heavy medium separation is suggested as a main beneficiation method for such an antimony ore.

Table 8. Summary of the simulation studies

Stream	% 10Sb Concentrate			% 12Sb Concentrate			% 14Sb Concentrate			% 16Sb Concentrate		
	tph	Grade (%)	Rec. (%)	tph	Grade (%)	Rec. (%)	tph	Grade (%)	Rec. (%)	tph	Grade (%)	Rec. (%)
Feed	20	1.18	100	20	1.18	100	20	1.18	100	20	1.18	100
Coarse Conc.	0.85	10.04	36.16	0.69	12.05	35.23	0.58	14.02	34.46	0.5	16.01	33.92
Fine Conc.	0.3	10.05	12.78	0.25	12.08	12.8	0.21	14.06	12.51	0.18	16.02	12.22
Total Conc.	1.15	10.04	48.94	0.94	12.06	48.03	0.79	14.03	46.97	0.68	16.01	46.14
Coarse Tail	14.9	0.48	30.31	15.06	0.49	31.27	15.17	0.5	32.14	15.25	0.5	32.31
Fine Tail	1.16	0.54	2.65	1.21	0.54	2.77	1.25	0.54	2.86	1.28	0.56	3.04
Slime	2.77	1.55	18.19	2.77	1.55	18.19	2.77	1.55	18.19	2.77	1.55	18.19
Tail+Slime Total	18.83	0.64	51.15	19.04	0.65	52.23	19.19	0.65	53.19	19.3	0.65	53.54

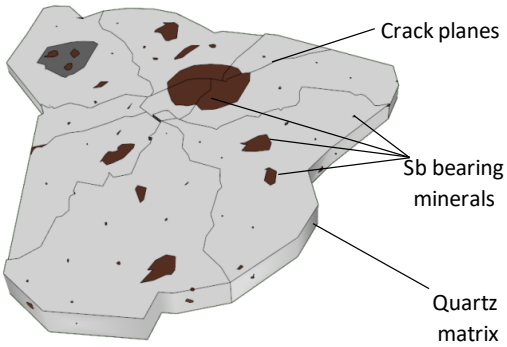

Fig. 13. Schematic representation of the mineralogy of the antimony ore

Based on the modelling scenarios discussed previously; a conjectural exemplary flowsheet (Figure 14) was proposed and mass-water balance was calculated by simulation studies in case of producing a concentrate with 12% Sb content. In Figure 14, the feed from crushing circuit was delivered via a spiral classifier to remove clay and very fine material. Then, the material was screened through 0.5 mm screen to remove remaining fine material and water before heavy medium cyclone. +0.5mm material is fed to heavy medium cyclone. Both float (tailing) and sink (concentrate) products are taken on separate drain and rinse screens where ferrosilicon (ultra-fine material used for density adjustment) is recycled and recovered. Those streams are displayed with the dashed red lines in Figure 14. A magnetic separator was placed in the flowsheet to recover the medium from diluted streams coming from drain and rinse screens. As the major part of the water was obtained from the tail of the magnetic separator, some part of it was recirculated as the spray water and excess of it was send to thickener. Coarse concentrate and tail had little water, while fine concentrate had 71% of solids which can be further dewatered at the existing concentrate pool. -0.5 mm is fed to hydraulic classifier (hydrosizer) which classifies material into size and (some extend) density classes. The underflow of first compartment consists of coarse particles as well as fine dense particles utilizing a convenient feed material for shaking tables. In the first stage shaking table operation, high recovery should be aimed rather than upgrading and in the

second stage, expected final upgrading degree will be achieved. Second stage tailings will be recycled to first stage feed to maximize the recovery. Consequently, best possible processing flowsheet in detail was designed based on the experimental results and mineralogical properties exclusively for the subjected complex antimony ore.

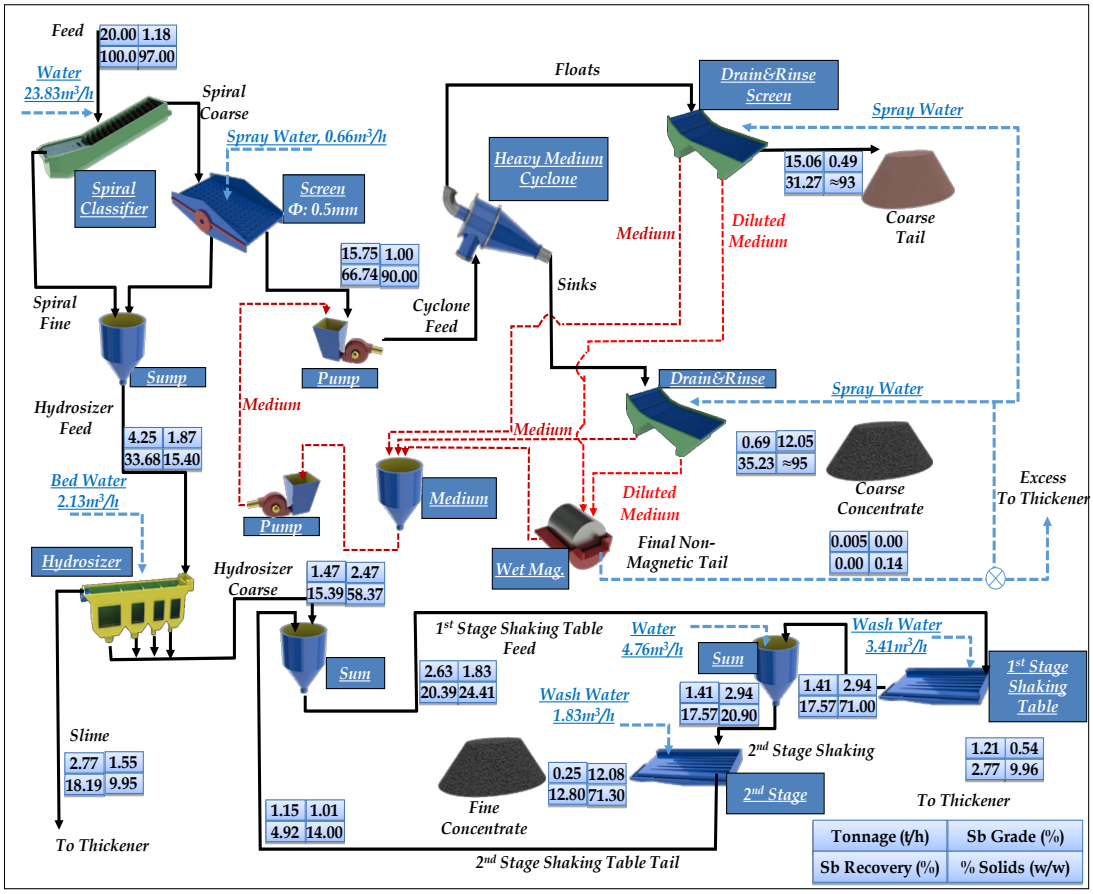

Fig. 14. Mass-water balance in case of producing a concentrate with 12% Sb content

4. Conclusions

Antimony ores are known for their lack of the response to many enrichment methods due to the common complex mineralogy, tendency to team up with clayey content forming a problematic slime fraction, and low initial head grades. Therefore, this study was dedicated to detail investigation of an antimony ore in terms of mineralogy, beneficiation, and resulting plant design strategies. Considering the unique properties of the antimony subjected to this study, following conclusions were underlined within the most general terms;

- Antimony ore did not respond well to investigated beneficiation methods other than heavy medium separation.
- The sample used in the experimental studies contained about 1% Sb and it was best possible to obtain a concentrate having 10-12 %Sb with a concentration ratio of 17-21.
- Since the ore mineralogy drives totally different beneficiation behaviors, the mineralogical variability of the subjected antimony ore had been proven to be the most critical aspect and should be considered in detail when a sustainable plant design effort was considered.

References

ANDERSON G.C., 2012. *The metallurgy of antimony*. Chemie der Erde. 72, S4, 3–8.

BAUM, W., 2014. *Ore characterization, process mineralogy and lab automation a roadmap for future mining*. Minerals Engineering 60, 69–73.

BOSMAN, J., 1998. *Dense medium Separation-Does size really count.* 6th Samancor Symposium-Dense Media'97, Broome, Western Australia AC Partridge and IR Partridge (Eds), Paper C2.

BUTTERMAN, W.C., CARLIN, J.F., 2004. *Mineral commodity profiles, antimony.* Open-File Report 03-019US. Department of the Interior, US Geological Survey.

CARDARELLI F.(Ed.), 2008. *Materials Handbook-A Concise Desktop Reference.* Springer-Verlag London Limited. 2nd Edition. ISBN-13: 9781846286681. 1340 pages.

DU, X., QU, F., LIANG, H., LI, K., YU, H., BAI, L., LI, G., 2014. *Removal of antimony (III) from polluted surface water using a hybrid coagulation–flocculation–ultrafiltration (CF–UF) process.* Chemical Engineering Journal 254, 293–301.

FIGI, R., NAGEL, O., TUCHSCHMIDA, M., LIENEMANNA, P., GFELLER, U., BUKOWIECK, N., 2010. *Quantitative analysis of heavy metals in automotive brake linings: A comparison between wet-chemistry based analysis and in-situ screening with a handheld X-ray fluorescence spectrometer.* Analytica Chimica Acta 676, 46–52.

FILELLA, M., BELZILE, N., CHEN, Y.W., 2002. *Antimony in the environment: a review focused on natural waters - I. Occurrence.* Earth-Science Reviews 57, 125–176.

GAD, S. C., 2014. *Antimony.* Encyclopedia of Toxicology (Third Edition). Pages 274-276.

GORDON, H.P and HEUER, T. 2000. *New age radiometric ore sorting – the elegant solution. In: Proceeding of the Int. symposium of process metallurgy of uranium.* Saskatchewan 2000, Ozberk E., Oliver, A.J. (eds.) 323-337.

GUPTA, A., YAN, D.S., 2006. *Mineral Processing Design and Operations.* Amsterdam: Elsevier, p516.

GÜLCAN, E., GÜLSOY, Ö. Y., 2018. *Optical sorting of lignite and its effects on process economics.* International Journal of Coal Preparation and Utilization, 38:3, 107-126, DOI: 10.1080/19392699.2017.1383247.

HENCKENS, M.L.C.M., DRIESSEN, P.P.J., WORRELL, E., 2016. *How can we adapt to geological scarcity of antimony? Investigation of antimony's substitutability and of other measures to achieve a sustainable use.* Resources, Conservation and Recycling 108, 54–62.

LAGER, T., FORSSBERG, K.S.E., 1989a. *Beneficiation characteristics of antimony minerals a review- part 1.* Minerals Engineering Volume 2, Issue 3, Pages 321-336

LAGER, T., FORSSBERG, K.S.E., 1989b. *Current processing technology for antimony-bearing ores a review, part 2.* Minerals Engineering Volume 2, Issue 4, Pages 543-556.

LIDE, D.R. (Ed.), 2007. *The Elements. CRC Handbook of Chemistry and Physics,* 87th ed., Taylor and Francis, Boca Raton, Florida.

LOTTER, N. O., 2011. *Modern Process Mineralogy: An integrated multi-disciplined approach to flowsheeting.* Minerals Engineering 24, 1229–1237.

LOTTER, N.O., BAUM, W., REEVES, S., ARRUÉ, C., BRADSHAW, D.J., 2018. *The business value of best practice process mineralogy.* Minerals Engineering Volume 116, Pages 226-238.

LOTTER, N.O., KORMOS, L.J., OLIVEIRA, J., FRAGOMENI, D., WHITEMAN, E., 2011. *Modern Process Mineralogy: Two case studies.* Minerals Engineering 24, 638–650.

MANSER, R.J., BARLEY, R.W., WILLS, B.A., 1991. The shaking table concentrator — The influence of operating conditions and table parameters on mineral separation — The development of a mathematical model for normal operating conditions, Minerals Engineering Vol. 4 Issues 3–4, 369-381.

MINZ, F., BOLIN, N.J., LAMBERG, P., WANHAINEN, C., 2013. *Detailed characterization of antimony mineralogy in a geometallurgical context at the Rockliden ore deposit, North-Central Sweden.* Minerals Engineering 52, 95–103.

MULAR, A. L., HALBE D. N., BARRATT D. J., 2002. *Mineral processing plant design, practice, and control proceedings,* 2422. New York: SME.

MULTANI, R.S., FELDMANN, T., DEMOPOULOS, G.P., 2016. *Antimony in the metallurgical industry: A review of its chemistry and environmental stabilization options.* Hydrometallurgy 164, 141–153.

QI, Z., JOSHI, T. P., LIUA, R., LI, Y., LIUB, H., QU, J., 2018. *Adsorption combined with superconducting high gradient magnetic separation technique used for removal of arsenic and antimony.* Journal of Hazardous Materials 343, 36–48.

RAWAT, J.P., SINGH, D.K., 1976. *Synthesis, ion–exchange properties and analytical applications of iron(III) antimonate.* Anal. Chim. Acta 87, 157–162.

SCINICARIELLOA F., BUSERA, M. C., FEROEB, A. G., ATTANASIO, R., 2017. *Antimony and sleep-related disorders: NHANES 2005–2008*. Environmental Research 156, 247–252.

United States Environmental Protection Agency (USEPA), 1979. *Toxics release inventory, Doc. 745-R-00–007*, Washington, DC, USA.

VON KETELHODT, L., 2009. *Viability of optical sorting of gold waste rock dumps.* World Gold Conference 2009, The Southern African Institute of Mining and Metallurgy.

WHITEN, W.J., 1966. *Winter School on Mineral Processing*. Dept. of Min. and Met. Eng, The University of Queensland, Australia.

WHITEN, W. J., 1972a. *The simulation of crushing plants with models developed using multiple spline regression.* 10th Int. Symp. on the Application of Computer Methods in the Min. lnd, Johannesburg, 317–23.

WHITEN, W.J., 1972b. *Simulation and Model Building for Mineral Processing.* PhD Thesis, The University of Queensland, Australia.

WILLS, B. A., FINCH, J., 2015. *Wills' mineral processing technology: An introduction to the practical aspects of ore treatment and mineral recovery.* Butterworth-Heinemann 512:417–437.

WOTRUBA, H., 2006. *Sensor sorting technology – is the minerals industry missing a chance*. XXIII International Mineral Processing Congress, Vol.1, September 3-8.

WU, Z., HE, M., GUO, X., ZHOU, R., 2010. *Removal of antimony(III) and antimony(V) from drinking water by ferric chloride coagulation: competing ion effect and the mechanism analysis.* Sep. Purif. Technol. 76 (2), 184–190.

YELLISHETTY, M., HUSTON, D., GRAEDEL, T.E., WERNER, T.T., RECK, B.K., MUDD, G.M., 2017. *Quantifying the potential for recoverable resources of gallium, germanium and antimony as companion metals in Australia.* Ore Geology Reviews 82, 148–159.

ZHU, J., WU, F., PAN, X., GUO, J., WEN, D., 2011. *Removal of antimony from antimony mine flotation wastewater by electrocoagulation with aluminum electrodes.* Journal of Environmental Sciences, 23(7) 1066–1071.